Future Journal of Pharmaceutical Sciences

RESEARCH

Open Access

Nanoemulsion drug delivery system loaded with imiquimod: a QbD-based strategy for augmenting anti-cancer effects

Shital Tanaji Jadhav[1,2*], Vijay Rajaram Salunkhe[1] and Somnath Devidas Bhinge[1]

Abstract

Background Skin cancer is becoming a public health concern due to increased exposure to environmental pollutants and UV rays, among other factors. In India, skin neoplasms constitute 2–3% of all human cancer cases, whereas in the USA, 2–3 million cases of non-melanoma skin cancer are reported annually. Various drugs are available in the market for treating skin cancer. Imiquimod (IMQ) is one such drug approved by the USFDA for managing basal cell malignancy, external genital warts, and actinic keratosis. The conventional dosage form of IMQ cream has several side effects that can lead to therapy interruption. Therefore, the present work aims to develop an IMQ nanoemulsion with improved solubility, in vitro drug release and stability. Nanoemulsion was formulated using oleic acid/rose oil, with polysorbate 20/propylene glycol selected as the oil phase and Smix, respectively. Optimization carried out using a 3^2 factorial design with the aid of a quadratic model. Characterization was conducted for parameters, namely viscosity, pH, drug content, globule size, zeta potential and entrapment efficiency. Thermodynamic stability studies were conducted to assess the stability of the formulation. Furthermore, the optimized system was subjected to TEM analysis, in vitro drug release and in vitro cytotoxicity assay (MTT assay).

Results Nanoemulsions were found to be in the size range of 152.80–470.13 nm and exhibited a spherical shape. Zeta potential values ranged from − 28.93 to − 58.48 mV. DSC measurements indicated the complete solubilization of IMQ in the nanoemulsion system. The optimized formulation F1 displayed the following characteristics: a globule size < 200 nm, a zeta potential > − 55 mV, a polydispersity index < 0.2, % drug content of 102.89 ± 1.06, % entrapment efficiency of 97.59 ± 0.24, a pH of 4.77 ± 0.06, and a viscosity of 4.06 ± 0.06 poise. In vitro IMQ release studies of nanoemulsion and commercial cream showed approximately 70% and 34% drug release, respectively, at the end of 8 h. Moreover, the in vitro cytotoxicity assay depicted that *F*1 exhibited greater cytotoxic potential compared to the commercial formulation against the A431 cell line.

Conclusion The present investigation showed a significant improvement in in vitro drug release of the BCS class IV drug IMQ and enhanced cytotoxic activity against cancerous cells. IMQ-loaded nanoemulsion represents a promising vehicle for delivering treatment to the skin for treating skin cancer.

Keywords Nanoemulsion, Imiquimod, Optimization, Drug, Skin cancer, Cytotoxicity, Formulation, Anti-cancer, Stability, Topical, Globule size

*Correspondence:
Shital Tanaji Jadhav
jahdhavshital138@gmail.com
Full list of author information is available at the end of the article

Graphical abstract

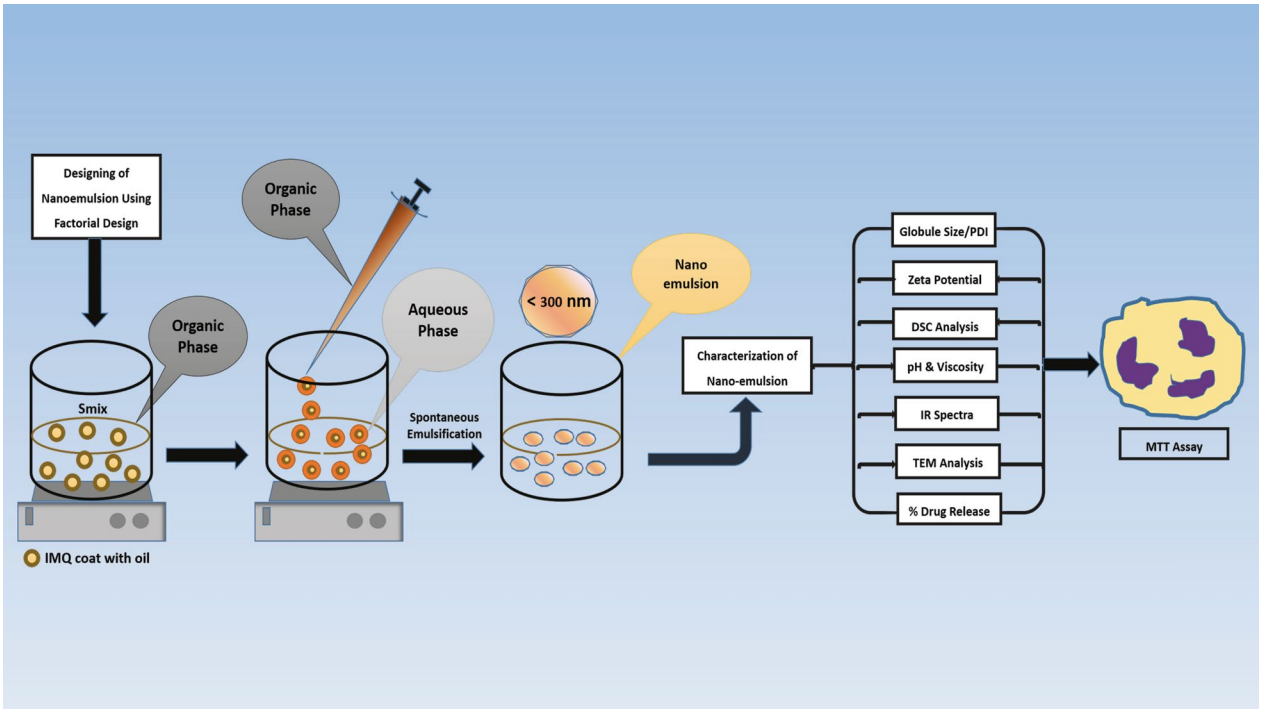

Background

Skin cancer is a growing global health concern due to increased exposure to environmental pollutants and UV rays, among other factors. In India, 2–3% of cases constitute skin neoplasm among all human cancers. Annually, around 2–3 million cases of non-melanoma skin cancer are found in the USA, representing more cases than all types of cancer combined [1]. Skin cancer is widely recognized as one of the most prevalent conditions affecting the human population, accounting for approximately 40% of all newly diagnosed cancer cases worldwide, according to findings from a literature survey [2].

IMQ was approved by the USFDA in 1997 for the therapy of external genital warts and further approved for actinic keratosis and basal cell carcinoma. IMQ exhibits properties as an immune response modifier, displaying potential anti-viral and anti-tumor effects in animal studies [3]. IMQ, an imidazoquinoline compound, functions as a low molecular mass immune modifier capable of locally enhancing several cytokines, such as interferon-alpha, tumor necrosis factor-alpha, interleukin (IL)-1, IL-6, IL-8, IL-12, among others. Enhancement of endogenous response can be achieved by the induction of innate and adaptive immune response with the aid of IMQ. It can upregulate the body's own natural anti-viral and anti-tumor cell response [4]. IMQ functions as an agonist for toll-like receptors TLR7 and TLR8, stimulating the production of proinflammatory cytokines through the activation of central transcription and the nuclear factor kappa (NF-κB) [5].

The nanoparticulated drug delivery system has been receiving emerging attention for the topical delivery system due to several advantages such as increased absorption through the skin, provision of sustained/prolonged action, and protection of encapsulated drug from degradation [6]. Nanoemulsions (NEs) consist of colloidal dispersions comprising an oil phase, an aqueous phase, a surfactant and a cosurfactant, balanced at suitable proportions. These are isotropic, thermodynamically stable and transparent system. These are kinetically stable emulsions with a droplet size range of 50–200 nm [7]. The maximum size of globules for topical drug delivery is 1000 nm [8]. The large surface area of nanoemulsions has the potential to enhance the rate of lipid digestion, assist in the release of bioactive substances, expedite the formation of mixed micelles, and improve the capacity of bioactive compounds to permeate through the mucus layer and epithelial cells [9]. Nanoemulsions have been explored as potential carriers for topical delivery vehicles due to their ability to penetrate deeper layers of the skin.

In recent years, topical drug delivery systems have gained significant attention due to their non-invasiveness and convenience in administering medications with both local and systemic effects, as compared to oral and parenteral methods [10, 11]. The outer layer of skin works as a barrier to drug penetration into deeper layers, making it a common target for efforts to enhance topical permeation ability.

The importance of employing the design of experiments in novel drug delivery systems cannot be overstated, as it allows for the systematic optimization of formulations, processes, and parameters. By utilizing statistical approaches, researchers can pinpoint critical factors that influence drug release, stability, and bioavailability, thereby leading to efficient resource utilization and maximizing drug delivery performance. Moreover, this methodology empowers researchers to grasp intricate interactions between formulation components, facilitating the development of safe, effective, and patient-friendly drug delivery systems. Essentially, the systematic application of design of experiments plays a central role in driving pharmaceutical research forward, expediting product development, and ultimately improving patient outcomes.

IMQ is a BCS class IV drug with a low molecular weight of 240.3 g/mol and poor penetrability. It exhibits low solubility in both hydrophilic and lipophilic solvents [12]. Hence, it is challenging to design the formulation for the topical delivery of the IMQ. Various adverse effects, such as itching, redness, and erythema at the site of application, have been reported with the conventional cream formulation of IMQ, which can result in therapy interruption [13, 14].

Therefore, the present investigation focuses on the development of IMQ NEs with improved solubility and permeation, as well as enhanced IMQ in vitro drug release to augment anti-cancer activity.

Materials and methods

IMQ was received as a gift sample from Ferror Healthtech, Interquim S A, Spain. Oleic acid, Propylene glycol and Lactic acid (98%) were obtained from Loba Chemie Private Limited, Mumbai. Rose oil was procured from Research Lab Fine Chem, Mumbai. Isopropyl Myristate, Polyethylene Glycol 400, Labrasol ALF, Polysorbate 20 and Medium Chain Triglycerides were provided as gift sample by Intas Pharmaceuticals Limited, Gujarat. The remaining chemicals and reagents used were of analytical quality.

Cell culture and media

The A431 cell line was obtained from NCCS Pune. Eagle minimum essential medium and antibiotic antimycotic 100X solution were obtained from Thermo Fisher Scientific Pvt Ltd, India. Earle's balanced salt solution was sourced from Gibco, USA, and Invitrogen, USA, and fetal bovine serum was also from Gibco, USA, and Invitrogen, USA.

Formulation design, optimization of IMQ NE

IMQ solubility in oils, surfactants and cosurfactants

The solubility of IMQ was confirmed by adding an excess quantity (500 mg) of IMQ to a capped vial containing 2 mL of various oils, surfactants and cosurfactants. The resultant solution was mixed with a vortex for 5 mints and then equilibrated at 37 ± 10 °C in an orbital shaker incubator for 48 h [15]. The supernatant samples were separated by centrifugation at 3000 rpm for 10 min and analyzed using a UV–visible spectrophotometer at 243.50 nm.

Pseudo ternary phase diagram

The phase diagram of oil, water, and Smix was created using an aqueous titration technique [16]. The oil phase was a combination of oleic acid and rose oil, while the Smix was composed of a solution of polysorbate 20 and the cosurfactant propylene glycol. Specific Smix ratios of 1:1 and 2:1 were employed in the study. Various fixed proportions of Oil: Smix were used, including 9:1, 8:2, 7:3, 6:4, 5:5, 4:6, 3:7, 2:8, and 1:9. Water addition was continued drop by drop with magnetic stirring at 400 rpm, and end point was determined through visual inspection of the mixture [17, 18].

Formulation and optimization of IMQ-loaded nanoemulsion

The drug-loaded nanoemulsion was prepared using the spontaneous emulsification method with minor modifications [19]. IMQ was completely dissolved in the prepared oil phase with the addition of 0.83% w/w lactic acid with magnetic stirring for 45 min. Subsequently, Smix was added to the IMQ-loaded oil while continuing to stir with a magnet. The resulting solution was added dropwise to an ample amount of distilled water containing 0.5% w/w lactic acid while being stirred magnetically at 710 rpm. Formulations were prepared by varying the concentration of oil and surfactant, as indicated in Table 1. The prepared nanoemulsions *F*1–*F*9 (Fig. 1A) were allowed to equilibrate for 24 h and subsequently characterized for various parameters.

A 3^2 factorial design was employed using Design Expert® software (Version 13.0, Stat-Ease Inc., USA) for the development of IMQ nanoemulsion. The impact of two independent variables, namely *X*1 (% oil concentration) and *X*2 (% Smix concentration) was explored with regard to globule size (*Y*1) and zeta potential (*Y*2). The

Table 1 Formulation batches of nanoemulsions

Ingredients % w/w	*F1*	*F2*	*F3*	*F4*	*F5*	*F6*	*F7*	*F8*	*F9*
IMQ	3.50	3.50	3.50	3.50	3.50	3.50	3.50	3.50	3.50
Oleic acid	15.00	15.00	12.50	12.50	17.50	15.00	17.50	17.50	12.50
Rose oil	3.00	3.00	2.50	2.50	3.50	3.00	3.50	3.50	2.50
Polysorbate 20	27.00	23.50	23.50	27.00	30.50	30.50	27.00	23.50	30.50
Propylene glycol	27.00	23.50	23.50	27.00	30.50	30.50	27.00	23.50	30.50
Lactic acid	1.33	1.33	1.33	1.33	1.33	1.33	1.33	1.33	1.33
Double distilled water (q.s)	100.00	100.00	100.00	100.00	100.00	100.00	100.00	100.00	100.00
Oleic acid: Rose Oil	5:1	5:1	5:1	5:1	5:1	5:1	5:1	5:1	5:1
Surfactant: cosurfactant	1:1	1:1	1:1	1:1	1:1	1:1	1:1	1:1	1:1

influence of independent variables on the responses was studied using ANOVA (*F* Value). Table 2 displays the coded independent variables. Optimization was conducted while taking into account various analysis parameters, such as globule size, zeta potential, drug content, and % entrapment efficiency [18].

Characterization of IMQ nanoemulsion

Drug content

IMQ content of the nanoemulsion was determined by addition 150 mg of the sample to 100 mL 0.1 M HCL and appropriately diluting it with the same solution. The resulting dilutions were analyzed by a UV–visible spectrophotometer (Shimadzu Corporation Japan) at 243.50 nm.

% Entrapment efficiency

Entrapment efficiency was determined through centrifugation. The unentrapped IMQ, which is considered to be in the supernatant, was estimated by using a UV–visible spectrophotometer after dilutions with methanol [15].

$$\% \text{ Entrapment efficiency} = [\text{Amount of IMQ entrapment}/\text{Amount of IMQ taken}] \times 100$$

pH

The pH of nanoemulsions was verified using a digital pH meter (Make–Hanna instruments) [20]. Readings were taken in triplicates and expressed as the mean ± SD.

DSC

DSC thermograms of IMQ, blank nanoemulsion, and IMQ NE were conducted using a Mettler Toledo (Star SW 10) instrument to assess the compatibility of the IMQ with the excipients. Heating was carried out at a rate of 10 °C per minute with a temperature range from 25 to 300 °C, accompanied by a nitrogen purge at a flow rate of 100 mL per minute. Additionally, this prepared formulation (2 mg) was weighed and placed in aluminum pan, with an empty pan used as a reference for analysis [21].

Infrared spectroscopy

To examine the interaction of the IMQ with excipients and to analyze the functional group of IMQ, FTIR spectra were recorded in the range of 450–4100 cm^{-1}. The IMQ and physical mixtures were placed on a sample holder and analyzed by ATR FTIR spectrophotometer (Bruker, Japan).

Globule size and size distribution

The globule size and size distribution of the IMQ-loaded nanoemulsion were assessed by using a Particle size-Zeta potential analyzer (HORIBA scientific SZ 100, Japan) based on dynamic laser scattering. Size analysis was performed for 100 s at a detection angle of 90° [22].

Zeta potential

The zeta potential was measured using the HORIBA scientific SZ 100. The nanoemulsion was additionally diluted with deionized distilled water at a ratio of 1:100 and transferred into a transparent disposable zeta cell. The measurement was conducted by allowing the sample to stand for 60 s.

Viscosity

A Brookfield rheometer was employed to assess the viscosity of the prepared nanoemulsion batches. Readings were taken at 100 rpm at 25 ± 2 °C.

Transmission electron microscopy (TEM)

The morphology of the IMQ NE surface was visualized with TEM. The sample was placed on a carbon-coated metal grid (copper) and stained with a 1% w/v phosphotungstic acid solution. After air drying, the sample was

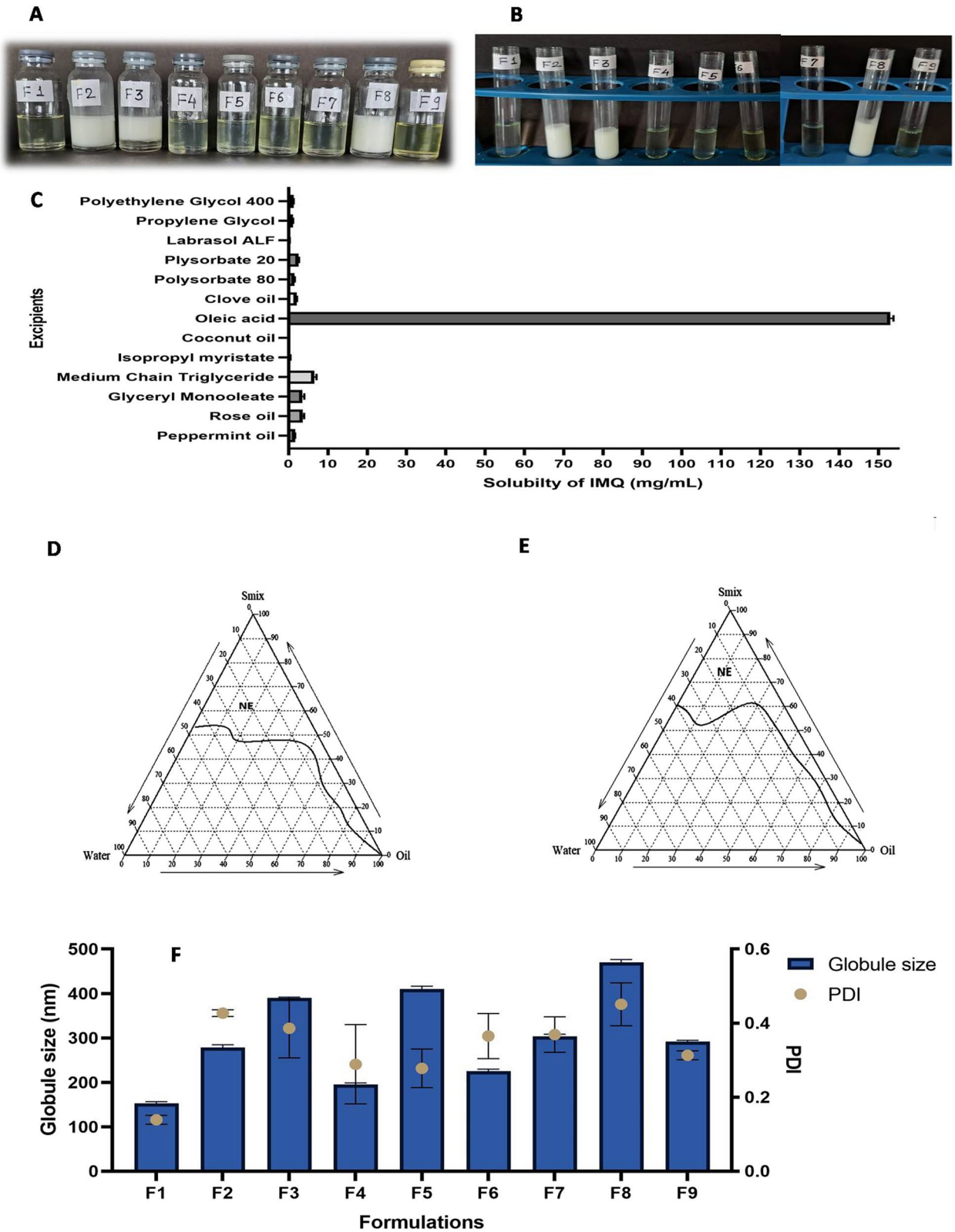

Fig. 1 **A** IMQ-loaded NEs, **B** NEs after thermodynamic stability testing, **C** Solubility of IMQ in oils, surfactant-cosurfactants, **D**, **E** Pseudoternary phase diagram of Smix 1:1, 2:1. **F** Globule size and PDI of IMQ NE

Table 2 Variables in 3^2 factorial design

Independent variable	Levels used		
	−1	0	+1
*X*1: % Oil concentration	15	18	21
*X*2: % Smix concentration	47	54	61
Response: dependent variable			
*Y*1 Globule size in nm	Minimum		
*Y*2 Zeta potential in mV	Maximum		

observed under a high-resolution TEM (JEM 2100F, JEOL Ltd) at 200 kV [23].

Thermodynamic stability

Thermodynamic stability was evaluated based on the following parameters.

Freeze thaw cycle

The prepared nanoemulsion batches were stored at −21 °C for 24 h After the complete 24 h, the nanoemulsions were brought to ambient temperature. This process was repeated for 6 cycles. Nanoemulsions with good stability returned to original state within 2–3 min [15].

Centrifugation

Phase separation in nanoemulsions was assessed through a centrifugation test. Five-gram samples were placed in a tube and centrifuged at 3500 rpm for 15 min and the results were observed visually.

Heating cooling cycle

After the centrifugation test, the nanoemulsions were subjected to a heating cooling cycle. For the cooling cycle, a temperature of 4 °C was maintained, and for the heating cycle, the temperature was held steady at 45 °C for a continuous 48 h. Six cycles were repeated to assess thermal stability [15].

In vitro

For the in vitro IMQ release study, a Franz diffusion cell apparatus (Dolphin) with a volume of 25 mL and an area of 4.95 cm^2 was used. A dialysis membrane was employed to separate the donor and acceptor compartment. The donor compartment was loaded with commercial Imiquad cream and IMQ-loaded optimized NE equivalent to 12.50 mg of IMQ. The acceptor compartment was filled 0.1 M HCl and allowed to stir continuously at 400 rpm [24]. Aliquot samples were withdrawn at specific time periods viz., 1,2,3,4,5,6,7 and 8 h and an equal portion of a fresh similar solution was regularly added to maintain the volume in the sink [20]. Appropriate dilutions were made with 0.1 M HCl and analyzed by a UV–visible spectrophotometer at 243.50 nm.

$$\begin{aligned}&\text{Cumulative amount of drug release}\\&=\left[\text{Concentration}\left(\mu\text{g/mL}\right)\right.\\&\quad\times\text{volume of diffusion medium}\\&\quad\left.\times\text{dilution factor}\right]/1000\end{aligned}$$

The release kinetic profiles were assessed using mathematical models, namely Zero order, First order, Higuchi and Korsmeyer–Peppas. The equations used for mathematical models are mentioned in Eqs. (1) to (4) [25–27]

$$\text{Zero order}\quad Q = K_o t \tag{1}$$

Q: amount of drug released at time *t*, K_o: zero-order rate constant, *t*: time in hrs.

$$\text{First order}\quad \text{Log}\, Q_t = Log\, Q_o + [Kt/2.303] \tag{2}$$

Log $Q_{t:}$ Drug amount remaining to be released at time *t*, Log Q_o: Drug amount remaining to be released at zero hr, *K*: Release rate constant.

$$\text{Higuchi}\quad Q = K_H t_{1/2} \tag{3}$$

Q is amount of drug released at time *t*, K_H is release rate constant.

$$\text{Korsmeyer}-\text{peppas}\quad M_t/M_\infty = Kt^n \tag{4}$$

M_t = amount of drug released at time *t*, M_∞ $M\infty$ = amount of drug released at infinite time. M_t/M_∞ = fraction of drug release, *n* = diffusion exponents.

In vitro cytotoxicity assay

The impact of the optimized IMQ NE on the cancerous cell line A431 was evaluated using the MTT assay [24, 28–31]. The chosen cells were placed in an incubator at a fixed concentration of 1×10^4 cells/mL in a culture medium for a complete one day at 37 ± 2 °C and 5% CO_2. The cells were seeded at a selected concentration of 70 µL (1×10^4 cells) per well in 100 µL of culture medium. In separate wells of the microplate, 100 µL of the optimized IMQ NE and Imiquad cream samples were added, respectively. A culture grade microplate with 96 wells was utilized. Control wells were also incubated with selected solution of DMSO (0.2% in PBS) and the cell line. This was performed to quantify the survival of control cells and the % of live cells after culture. All samples were incubated in triplicate. The cell cultures were incubated for an additional complete one day at 37 °C and 5% CO_2 in a CO_2 incubator (Thermo Scientific BB150). After the incubation period, the medium was completely removed, and 20 µL of 5 mg/ml MTT reagent (in PBS) was added

to each well. The treated cells were subsequently incubated with MTT for a continuous 4 h while maintaining a temperature of 37 °C in the CO_2 incubator. The wells were observed under a microscope for the formation of formazan crystals. The yellow colored MTT dye was reduced to an intensely colored formazan only by viable cells. Finally, after completely removing the medium, 200 µL of DMSO was added to each well, and then, the plate was re-incubated for a continuous 10 min. The plate was covered with aluminum foil during this step. IMQ samples were quantified by measuring the absorbance of each selected sample using a microplate reader (Benesphera E21) at a selected wavelength of 550 nm.

Statistical analysis

One-way ANOVA was utilized as a statistical tool to determine statistical significance. GraphPad prism (Trial version 9, Boston MA) was employed for the analysis. Significant results were recorded when $p < 0.05$ at 95% confidence interval.

A multiple comparison post hoc Tukey's test was used to confirm significant difference among the test groups.

Results

IMQ solubility in oils, surfactants and cosurfactants

IMQ is highly insoluble in aqueous media [12]. During the formulation development of the nanoemulsion, the solubility of IMQ in different oils (clove oil, oleic acid, coconut oil, oleic acid, isopropyl myristate, medium chain triglyceride, glyceryl monooleate, rose oil, peppermint oil) and surfactant-cosurfactants (polysorbate 80, 20, Labrasol ALF, propylene glycol, poly ethylene glycol 400) was assessed, as shown in Fig. 1C. Among the different oils screened, oleic acid exhibited the highest solubility (153.03 mg/mL). Rose oil had a solubility of 3.33 mg/mL and was used in combination with oleic acid. Polysorbate 20 was chosen as the surfactant because it demonstrated a high drug solubility of 2.60 mg/mL. Propylene glycol was selected as the cosurfactant due to its high capacity to solubilize the drug and compatibility with polysorbate 20.

Pseudo ternary phase diagram

It shows the existence of monophasic and biphasic dispersion system formed from distinct sets or combination of different proportions of ternary components comprising Smix, water, and the oil blend [32]. The pseudoternary phase diagram revealed both transparent nanoemulsion and a turbid coarse dispersion region [33]. Phase diagrams were plotted for 1:1 and 2:1 surfactant to cosurfactant ratio. The nanoemulsion region was identified and a 1:1 Smix was optimized with the maximum emulsification region (Fig. 1D, E).

Formulation and optimization of IMQ-loaded nanoemulsion

A 3^2 full factorial design was employed to design the nanoemulsions. Contour plot and 3D response graphs were used to illustrate the influence of the concentration of the oil phase (*X*1) and the concentration of Smix on globule size (*Y*1) and zeta potential (*Y*2). The size of globule and zeta potential are presented in Table 3. They were found to be in the range of 152.80–470.13 nm and −28.93 to −58.48 mV, respectively. The best fitted model for globule size and zeta potential was the quadratic model (Tables 4 and 5). All formulations

Table 3 3^2 factorial design matrix and results of responses

Std	Run	*X*1 A: Oil concentration %	*X*2 B: Smix concentration %	*Y*1 Globule size nm	*Y*2 Zeta potential mV
5	1	18	54	152.80 ± 3.62	−58.93 ± 0.50
2	2	18	47	279.00 ± 5.56	−47.80 ± 1.25
1	3	15	47	390.00 ± 2.00	−28.93 ± 1.20
4	4	15	54	194.73 ± 3.98	−35.23 ± 0.93
9	5	21	61	410.20 ± 6.21	−39.83 ± 1.44
8	6	18	61	225.83 ± 3.99	−58.48 ± 1.85
6	7	21	54	303.63 ± 4.72	−30.40 ± 1.24
3	8	21	47	470.13 ± 6.18	−26.56 ± 1.76
7	9	15	61	292.30 ± 2.52	−42.30 ± 0.92

Values are expressed as mean ± SD

Table 4 Statistics summary for globule size and zeta potential

Source	SD	R^2	Adjusted R^2	Predicted R^2	PRESS	Remark
For globule size						
Linear	103.93	0.2628	0.0171	-0.7271	1.518E+05	
2FI	113.53	0.2669	−0.1730	−3.3887	3.858E+05	
Quadratic	18.54	0.9883	0.9687	0.8992	8863.57	Suggested
Cubic	27.91	0.9911	0.9291	−0.6146	1.419E+05	Aliased
For zeta potential						
Linear	12.44	0.2106	−0.0525	−0.5278	1796.96	
2FI	13.63	0.2106	−0.2630	−1.6219	3083.74	
Quadratic	3.08	0.9758	0.9355	0.8028	231.99	Suggested
Cubic	4.92	0.9794	0.8354	−2.7509	4411.62	Aliased

Table 5 Fit statistics for globule size and zeta potential

Parameters	Globule Size (nm)	Zeta potential (mV)
Standard deviation	18.54	3.08
Mean	302.07	−40.94
C.V.%	6.14	7.52
R^2	0.9883	0.9758
Adjusted R^2	0.9687	0.9355
Predicted R^2	0.8992	0.8028
Adeq precision	21.7165	14.0041

exhibited a polydispersity index (PDI) below 0.5, indicating a uniform distribution of globules (Fig. 1F).

The coefficient associated with each variable enabled a direct comparison of their impact on the globule size, as indicated by the direction and magnitude of their coefficients [13]. The obtained ANOVA results demonstrate the statistical significance ($p = 0.043$) of the factorial model for particle size, as represented by the following mathematical equation, at 95% confidence interval.

A positive sign in the polynomial equation indicates an increase in the response, whereas negative sign indicates a decline in the response due to the corresponding factor [18].

$$Y1 = +134.19 + 51.15X1 - 35.13X2 + 9.44X1X2 + 124.29X1^2 + 127.52X2^2$$

The particle size (Y1) was significantly affected by the concentration of the oil phase ($X1$) and the concentration of Smix. Globule size increased with an increase in oil concentration and decreased with Smix concentration. The interaction terms $X1$ and $X2$ for response $Y1$ were found to be insignificant ($p > 0.05$).

The ANOVA results confirm the statistical significance ($p = 0.0125$) of the factorial model for zeta potential, as represented by the following mathematical equation, at a 95% confidence interval.

$$Y2 = -55.65 + 1.61X1 - 6.22X2 + 0.0250X1X2 + 21.20X1^2 + 0.8700X2^2$$

For the full model, the predicted R^2 of 0.8992 is in reasonable agreement with the adjusted R^2 of 0.9687, the difference is less than 0.2 (Table 5). Adequate precision measures the signal-to-noise ratio. A ratio greater than 4 is desirable, and the obtained ratio of 21.7165 indicates an adequate signal. This model can be used to explore the design space.

Zeta potential ($Y2$) was significantly affected by the concentration of the oil phase ($X1$) and the concentration of Smix ($X2$). Zeta potential increased with increasing oil concentration and decreases with Smix concentration. The interaction terms $X1$ and $X2$ for response $Y2$ were found to be insignificant ($p > 0.05$). The 3D response surface plot (Fig. 2A–F) indicated that decreasing oil concentration and increased Smix concentration significantly reduced the globule size. However, increased oil concentration and Smix concentration significantly increased the zeta potential.

For the full model, the predicted R^2 of 0.802 is in reasonable agreement with the adjusted R^2 of 0.935, the difference is less than 0.2. Adequate precision measures the signal-to-noise ratio. A ratio greater than 4 is desirable, and the obtained ratio of 14.004 indicates an adequate signal. This model can be used to explore the design space.

Globule size and zeta potential are important parameters for nano drug delivery system. Hence, optimization of IMQ NE was carried out with consideration of analyzing parameter constrains such as maximum zeta

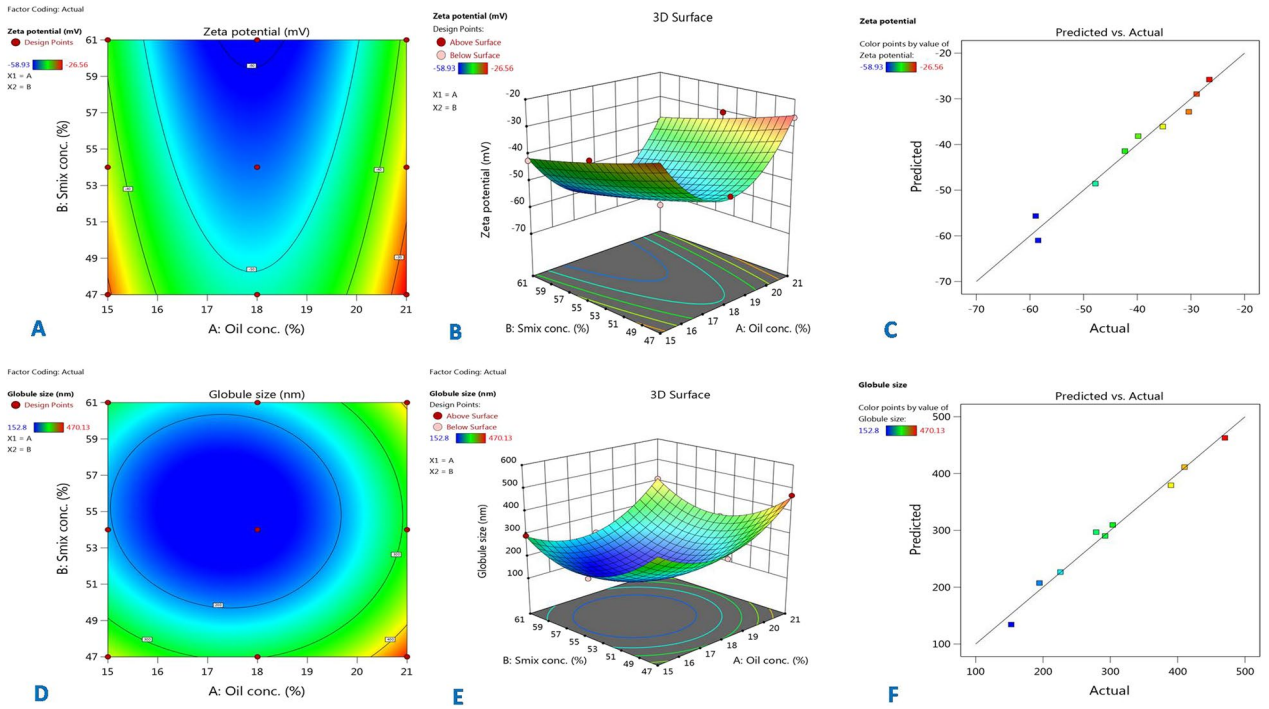

Fig. 2 **A**–**C** 3D response surface plot zeta potential. **D**–**F** 3D response surface plot for globule size

Table 6 Characterization of IMQ NEs

Formulation	Parameters				PDI
	Drug content (%)	% Entrapment efficiency	pH	Viscosity (Poise)	
*F*1	102.89 ± 1.06	97.59 ± 0.24	4.77 ± 0.06	4.06 ± 0.07	0.14 ± 0.01
*F*2	97.64 ± 2.36	91.11 ± 0.48	4.60 ± 0.10	1.32 ± 0.02	0.43 ± 0.01
*F*3	95.25 ± 1.80	90.63 ± 0.22	4.17 ± 0.12	1.11 ± 0.00	0.39 ± 0.09
*F*4	96.42 ± 1.65	92.81 ± 0.15	4.33 ± 0.06	1.76 ± 0.08	0.29 ± 0.11
*F*5	99.15 ± 0.98	98.03 ± 0.04	4.23 ± 0.06	6.46 ± 0.03	0.28 ± 0.05
*F*6	97.90 ± 1.48	93.21 ± 0.21	4.30 ± 0.10	4.21 ± 0.02	0.37 ± 0.06
*F*7	98.05 ± 1.48	95.54 ± 0.16	4.60 ± 0.10	2.92 ± 0.02	0.37 ± 0.05
*F*8	97.47 ± 2.13	94.01 ± 0.21	4.57 ± 0.06	1.22 ± 0.01	0.45 ± 0.06
*F*9	96.80 ± 1.92	93.01 ± 0.21	4.40 ± 0.10	5.30 ± 0.00	0.31 ± 0.01

Values are expressed as mean ± SD

potential, minimum globule size and optimum entrapment efficiency, drug content [18].

Characterization of IMQ nanoemulsion

Drug content

The IMQ content of the nanoemulsions was observed to be in the range of 96.42 ± 1.65% to 102.89 ± 1.06%. Table 6 shows a uniform distribution of IMQ. The concentration of oil and Smix showed a significant effect on the formulations.

% Entrapment efficiency

Nanoemulsions were characterized for % entrapment efficiency and were found to be in the range of 90.63 ± 0.217% to 97.59 ± 0.236% (Table 6). Nanoemulsion *F*1 showed the highest % entrapment efficiency of 97.59 indicating the good solubilization potential of the excipients.

pH and viscosity analysis

The pH of the nanoemulsion was observed to be around 4.5. The viscosity of the nanoemulsions ranged from 1.11

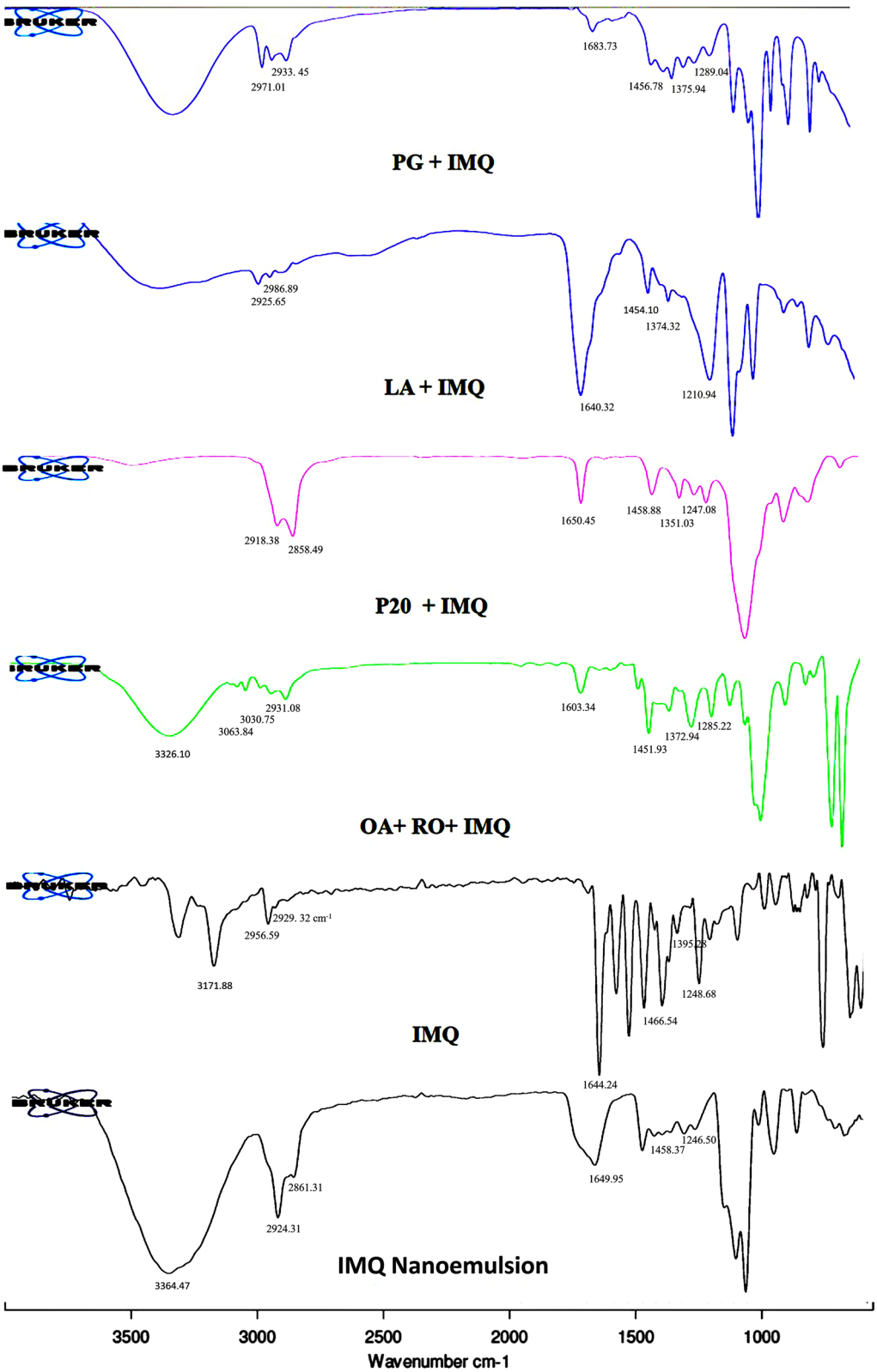

Fig. 3 DSC thermogram of IMQ, blank NE and IMQ NE

Poise to 6.46 Poise. The optimized batch F1 showed a viscosity of 4.06 Poise, which is sufficient to maintain the physical stability of the nanoemulsion. A significant difference was observed between formulations, indicating the impact of an increased concentration of Smix and oil.

DSC

The endothermic peak of IMQ was observed at 297.33 °C with a peak onset at 297.06 °C (Fig. 3), indicating the melting point of IMQ. Blank NE showed peaks at 90.92 °C, 183.63 °C, 300.38 °C due to surface oxidation. Optimized nanoemulsion F1 (IMQ NE) showed a peak at 129.13 °C with a peak onset at 128.96 °C indicating the solubilized form of IMQ in the nanoemulsion.

Infrared spectroscopy

IR of physical mixtures

The FTIR spectra of the physical mixture (Fig. 4) of IMQ and Propylene glycol showed characteristic peaks corresponding to various functional groups. These included N–H bending, C=N stretch (imine), CH_2 (alkane), CH_3, C–H stretch (aliphatic), and C–H stretch (aromatic) at specific wavenumbers of 1456.78, 1683.73, 1375.94, 1289.04, 2933.45, and 2971.01 cm^{-1}, respectively. Notably, the N–H stretch (primary amine) peak in the IMQ spectra merged with the formulation spectra due to the higher % transmission of the O–H peak caused by propylene glycol.

The FTIR spectra of the prepared physical mixture of oleic acid, rose oil and pure IMQ showed characteristic peaks corresponding to various functional groups. These included N–H stretch (primary amine), N–H bending, C=N stretch (imine), CH_2 (alkane), CH_3, C–H stretch (aliphatic), and C–H stretch (aromatic) at specific wavenumbers at 3063.84, 1451.93, 1603.34, 1372.94, 1285.22, 3030.75, and 2931.08 cm^{-1}, respectively.

The FTIR spectra of the prepared physical mixture of polysorbate 20 and pure IMQ showed characteristic peaks corresponding to various functional groups. These included N–H bending, C=N stretch (imine), CH2 (alkane), CH3, C–H stretch (aliphatic), and C–H stretch (aromatic) at specific wavenumbers of 1458.88, 1650.45, 1351.03, 1247.08, 2858.49, and 2918.38 cm^{-1}, respectively. Notably, the N–H stretch (primary amine) peak in the IMQ spectra merged with the formulation spectra due to the higher % transmission of the O–H peak caused by polysorbate 20.

The FTIR spectra of the prepared physical mixture of lactic acid and pure IMQ showed characteristic peaks corresponding to various functional groups. These included N–H bending, C=N stretch (imine), CH_2 (alkane), CH_3, C–H stretching (aliphatic) and C–H stretching (aromatic) at specific wavenumbers of 1454.10, 1640.32, 1374.32, 1210.94, 2925.65 and 2986.89 cm^{-1}, respectively. Notably, the N–H stretch (primary amine) peak in the IMQ spectra merged with the formulation

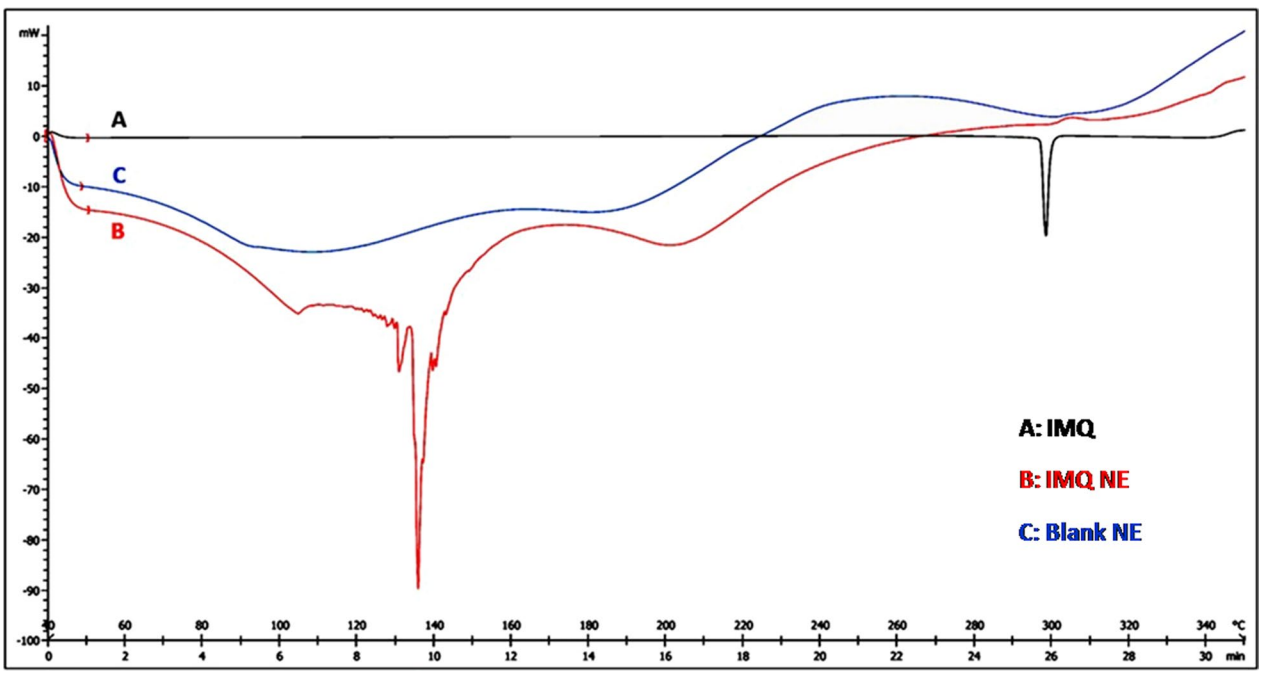

Fig. 4 FTIR analysis of physical mixture and IMQ NE

spectra due to the higher % transmission of the O–H peak caused by lactic acid.

IR of nanoemulsion

The FTIR spectra of IMQ showed characteristic peaks (Fig. 4) corresponding to various functional groups. These included N–H stretch (primary amine), N–H bending, C=N stretch (imine), CH_2 (alkane), CH_3, C-H stretching (aromatic), and C–H stretching (aliphatic) at specific wavenumbers at 3171.88, 1466.54, 1644.24, 1395.28, 1248.68, 2956.59, and 2929. 32 cm^{-1}, respectively, whereas the prepared formulations also exhibited similar functional groups, including N–H bending, C=N stretch (imine), CH_2 (alkane), CH_3, C–H stretching (aliphatic), C–H stretching (aromatic), and C=C (aromatic), at wavenumbers 1458.37, 1649.95, 1410.49, 1246.50, 2861.31, and 2924.31 cm^{-1}, respectively, when compared to the standard peaks.

Significantly, the N–H stretch (primary amine) peak in the IMQ spectra merged with the formulation spectra due to the higher % transmission of the O–H peak caused by propylene glycol. In general, the majority of the peaks maintained their positions when comparing the IR values of IMQ NE with the standard drug IMQ spectra.

Transmission electron microscopy

TEM images (Fig. 5) of the nanoemulsion revealed spherical-shaped globules with good dispersion and their sizes were size depicted in nm.

Thermodynamic stability

Thermodynamic stability is a crucial parameter for assessing the stability of nanoemulsions. The prepared nanoemulsions successfully withstood the centrifugation test (except batch *F*3), freeze thaw cycle and heating cooling cycle without exhibiting any signs of turbidity, phase separation or creaming (Fig. 1B). Passing the centrifugation test signifies the homogeneity and stability of the system [15].

In vitro IMQ release and kinetic profile

In vitro IMQ release from the optimized nanoformulation *F*1 was found to be 69.92%, whereas the commercial cream Imiquad exhibited 34.32% at the 8 h time point

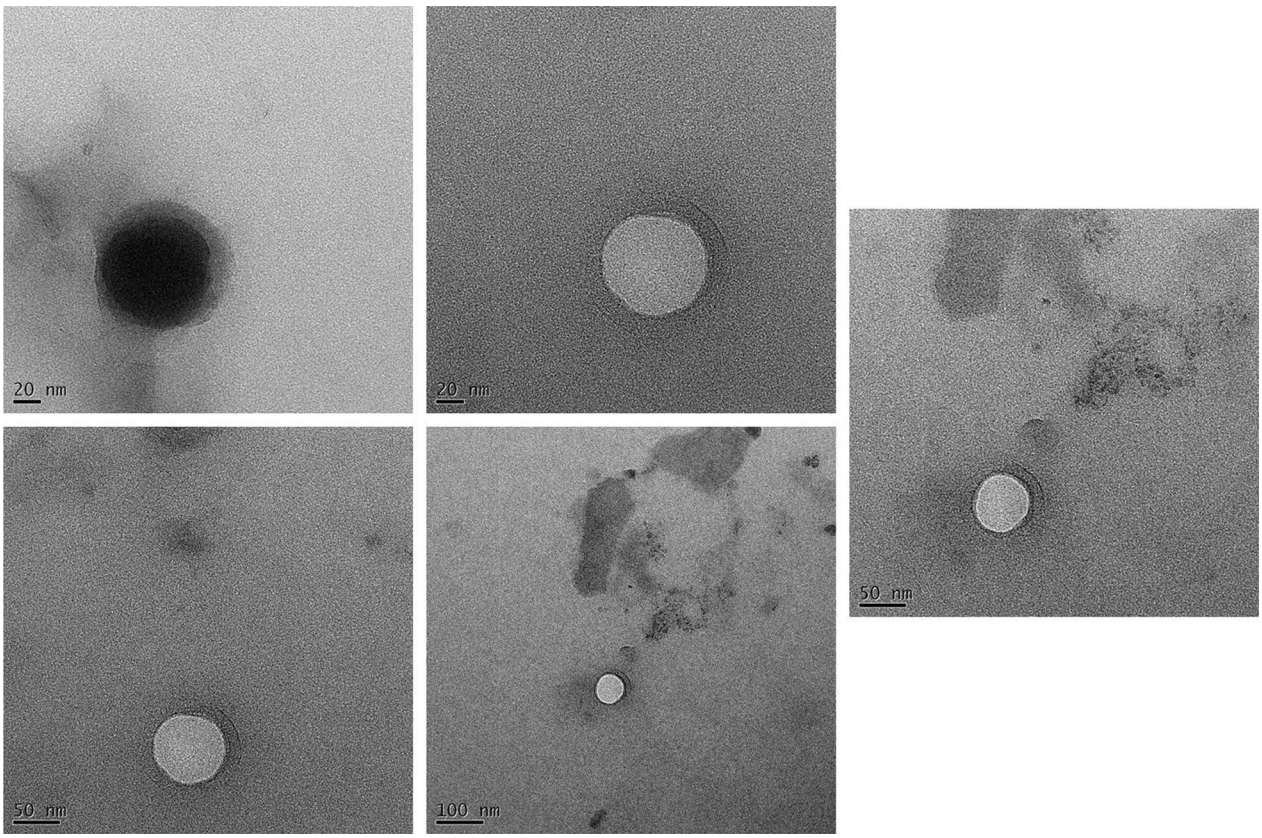

Fig. 5 TEM images of optimized IMQ NE

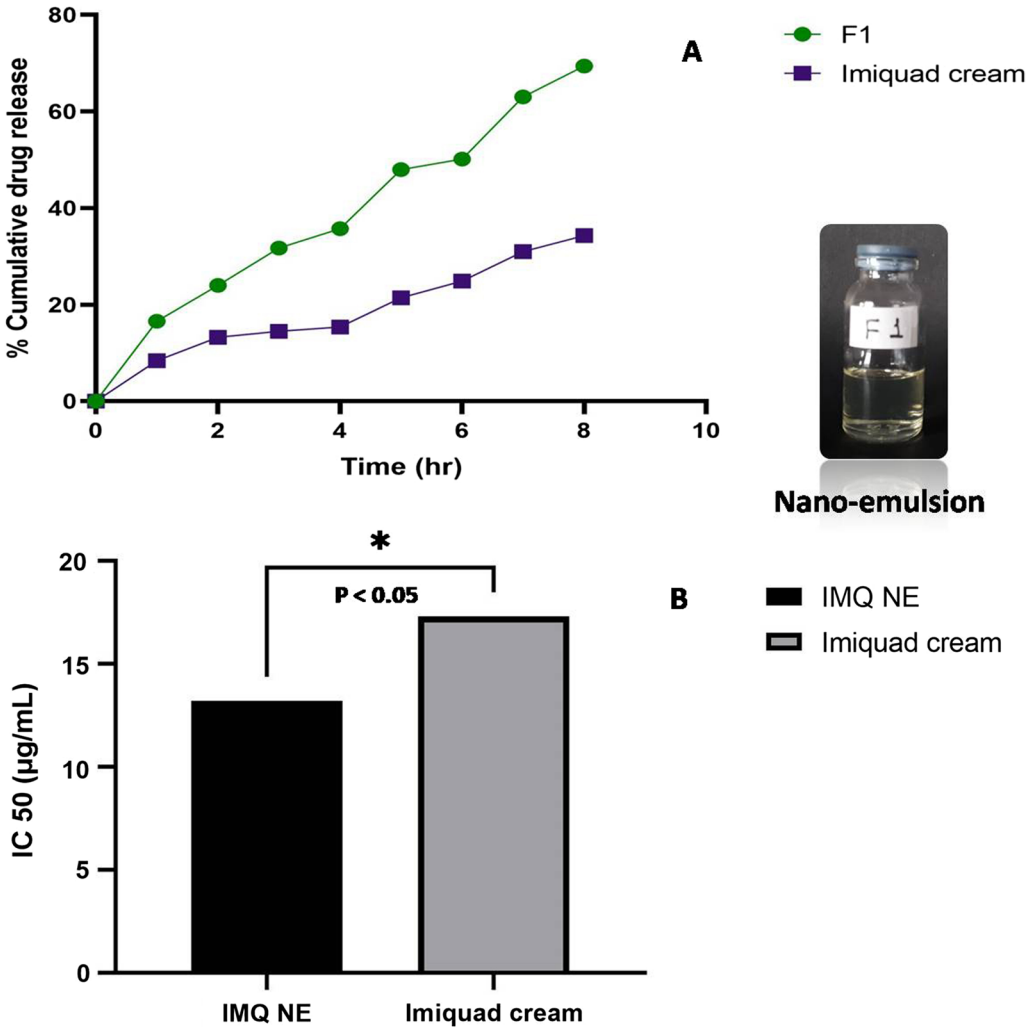

Fig. 6 **A** In vitro release of IMQ nanoemulsion **B** In vitro cytotoxicity assay of optimized IMQ NE

Table 7 In vitro IMQ release kinetics from optimized nanoemulsion and commercial formulation

Formulations	Zero order	First order	Korsmeyer peppas		Higuchi model
	r^2	r^2	r^2	*N*	r^2
F1	0.9817	0.9677	0.9796	0.690	0.9497
Imiquad cream	0.9693	0.9678	0.9369	0.655	0.9238

(Fig. 6A). A marked and highly significant difference exists between the nanoemulsion and the commercial cream with terms of % cumulative drug release (% CDR).

Kinetic models, as indicated in Table 7, were employed. The best-fitted model for both the nanoemulsion and the commercial cream was the zero order.

In vitro cytotoxicity assay

The optimized nanoemulsion was assessed for its anticancer potential by MTT assay on A431 cell lines. IMQ-loaded nanoemulsion showed an IC_{50} 13.20 ± 1.80 µg/mL, which was significantly different from the commercial cream (IC_{50} = 17.31 ± 1.08 µg/mL). Figure 6B illustrates that the nanoemulsion exhibits greater cytotoxic than Imiquad cream.

Discussion

In the proposed study, we optimized and developed IMQ NE using a low-energy emulsification technique. Nanoformulation excipients were selected based on solubility. The oil phase plays a vital role in the formation of nanoemulsions, serving to dissolve lipophilic drugs [16]. In our current research, we have primarily

utilized oleic acid to enhance the solubility of IMQ. Moreover, we chose rose oil due to its additional benefits, including anti-inflammatory, antioxidant effects, as well as its skin-healing properties, in addition to its solubilization capacity [34]. Incorporating rose oil along with oleic acid facilitated the solubilization of the drug. The multifaceted use of rose oil in nanoemulsions arises from its rich content of diverse bioactive compounds, such as terpenes, phenolics, and flavonoids, which offer potential skin benefits, including antioxidant, antiseptic, and anti-inflammatory properties [7]. Furthermore, its emollient properties help to moisturize and nourish the skin, maintaining its hydration and softness. Once drug along with oil incorporated into nanoemulsions, the reduced droplet size of the formulation has the potential to enhance the penetration of drugs into the skin. Therefore, a pseudoternary phase diagram was utilized to screen different proportions of oil, Smix and water with a larger nanoemulsification region. The gold standard for seeking optimized formulations has been the utilization of the response surface approach, which relies on quadratic modeling [35].

The factorial design comprising 9 runs (Table 3) suggested a quadratic model for the process optimization of formulations. However, out of the nine batches the *F*1 batch showed the minimum particle size (152.80 nm), the maximum zeta potential (−58.93 mV) (Table 3 and Fig. 7A–B), IMQ content (102.89%), and entrapment efficiency (97.59%). It has been taken as the optimized batch of IMQ nanoemulsion, consideration above analysis parameter constraints [18].

An increased concentration of Smix result in a reduction of interfacial tension within the oil phase and the aqueous phase, thus declining the free energy needed to reduce the size of the droplets into smaller size. An increased oil concentration at a specific Smix concentration had an impact on globule size. Excessive oil resulted in an increase in globule size in nanoemulsion batches. A polydispersity index below 0.5 indicated uniform globule dispersion and homogeneity in nanoemulsion system. The uniform distribution of globules confirms the even distribution of the IMQ in the formulation. TEM images indicated the spherical shape of globules in the optimized batch *F*1. A zeta potential of more than ± 30 mV provides good stability to the formulation [16]. The stability of a system is ensured by a high zeta potential, as adequately large charge can hinder particle aggregation due to the electrostatic repulsion within globules [36–38]. The observed result of the zeta potential of all batches indicated better stability for the prepared formulations. The magnitude of the zeta potential maintains the Brownian motion of globules. A negative zeta potential was obtained, which might be attributed to an electric charge on the globules, likely resulting from the types of ionizable moieties present and the pH of the aqueous phase. The high % entrapment efficiency of the optimized formulation *F*1 was due to the low surface tension within the droplets, which prohibited particles from coalescing together, as confirmed by the absence of any phase separation. This resulted in a high solubility of IMQ and its retention in the nanoemulsion system [37]. The optimum viscosity of 4.06 Pa was obtained, which is desirable to maintain the stability of the nanoemulsion. One-way ANOVA revealed a significant difference ($p < 0.05$) among the formulation batches in terms of particle size, zeta potential, IMQ content, % IMQ entrapment efficiency and viscosity. The statistical data confirm the significant impact of oil concentration and Smix on the above listed parameters.

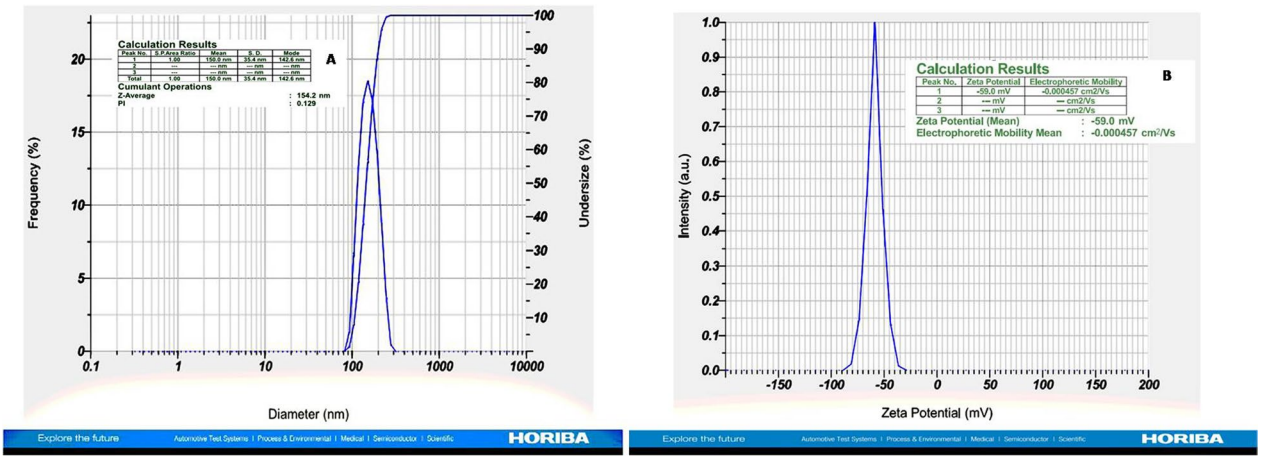

Fig. 7 **A** Globule size of IMQ NE, **B** Zeta potential of IMQ NE

The DSC thermogram of IMQ NE (Fig. 4) indicated the solubilization of the drug completely in the formulation, as no peak corresponding to the melting point of IMQ was observed. The initial endothermic peak in IMQ NE was observed as a straining hook. Molecular relaxation occurs due to the formation of an endothermic peak at 132.19 °C, followed by a further increase in mass due to oxidation. In case of blank nanoemulsion, multistage decomposition occurs up to 100 °C. The increase in mass after 100 °C is attributed to surface oxidation. Based on the interpretation of the IR data, there was no evidence of interaction between the selected excipients and IMQ in the physical mixture. Furthermore, the peak observed in the bulk IMQ was replicated in the nanoemulsion peak of IMQ, indicating that there were no interactions between the selected excipients and the IMQ, not only in the physical mixture but also in their formulation. Drug release is a critical characteristic of a therapeutic system, as it is essential for the absorption of the pharmacotherapeutic drug and plays a significant role in determining the amount and extent of active bioavailability to the body. The in vitro drug release study showed the release profile of *F*1 and the commercial cream Imiquad. It revealed a significant difference between *F*1 and Imiquad cream with respect to % CDR. The *F*1 formulation showed approximately a twofold increase in drug release compared to the equivalent drug in Imiquad cream. Decreased particle size with a low PDI enhanced the passage of IMQ through the cellophane membrane. Mathematical equation models are vital tools used to design formulations and calculate drug release processes in vitro and in vivo [39]. Through the kinetic analysis of the nanoemulsion formulation and Imiquad cream, it was observed that the release of IMQ follows a zero-order pattern, which does not differ from the commercial cream.

The kinetic study implies that the release is dictated exclusively by time and occurs at a uniform pace, unaffected by the concentration of the active ingredient. Nanoemulsion *F*1 exhibited significantly increased cytotoxicity toward the A431 cell line when compared to the commercial cream. The increased cytotoxicity may have been attributed to the smaller particle size allowing for greater penetration into the cell. The stability of a formulation is a crucial parameter to evaluate the quality of a product and its changes over time under the influence of different environmental parameters, such as temperature, humidity, light, and moisture. Moreover, nanoemulsions demonstrated thermodynamic stability with the aid of various parameters. Stability studies over 6 months confirmed the absence of creaming, cracking and turbidity in formulation, which was attributed to use of Smix with a specific ratio and the optimum concentration of the oil phase.

Conclusion

Our study revealed the potential application of IMQ in nanoemulsion form against skin cancer. It was formulated using 3^2 factorial design and optimized with considering analysis parameter constraints such as globule size, zeta potential, and drug content. IMQ nanoemulsions were developed from the nanoemulsion regions obtained from the pseudoternary phase diagram between oleic acid and rose oil (oil phase), polysorbate 20/propylene glycol (Smix) and water. The optimized nanoemulsion was validated using statistical parameter. IMQ NE significantly improved drug release in in vitro drug diffusion studies. Stability studies of IMQ NE confirmed this novel approach as a promising carrier for the topical delivery of IMQ. Additionally, in vivo research is necessary to analyze the acquired findings.

Abbreviations

IMQ	Imiquimod
Smix	Surfactant and cosurfactant mixture
NEs	Nanoemulsions
DMSO	Dimethyl sulfoxide
UV	Ultra-violet
IL	Interleukins
DSC	Differential scanning calorimetry
FTIR	Fourier transform infrared spectroscopy
TEM	Transmission electron microscopy
BCS	Biopharmaceutics classification system
PBS	Phosphate buffer saline
OA	Oleic acid
RO	Rose oil
PG	Propylene glycol
P20	Polysorbate 20
PDI	Poly dispersity index
SD	Standard deviation
ANOVA	Analysis of variance
hrs	Hours
rpm	Rotations per minute
min	Minutes
MTT	3-(4,5-Dimethylthiazol-2-yl)-2,5-diphenyltetrazolium bromide)
CDR	Cumulative drug release
USA	United States
FDA	Food and Drug Administration
NCCS	National Centre for Cell Science
IIT	Indian Institute of Technology

Acknowledgements

The authors would like to extend their sincere gratitude to the following individuals and organizations for their invaluable contributions and support to this research project: Ferror Healthtech, Interquim, Spain, for providing the gift sample of IMQ, Intas Pharmaceutical Pvt Ltd, Ahmadabad, for supplying gift samples of some excipients, IIT Mumbai, for conducting TEM analysis of the samples, Management and Principal, Annasaheb Dange College of B Pharmacy, Ashta, Maharashtra, India, for granting permission to use their research facilities, and Rajarambapu College of Pharmacy, Kasegaon, for their support throughout this research endeavor.

The assistance and generosity of these individuals and institutions have played a significant role in the successful completion of this study.

Author contributions
SJ contributed to study design, optimization of study, methodology, and writing—original draft; VS contributed to conceptualization and supervision, and review of manuscript; SB contributed to writing—original draft, review editing, and approval of final version.

Funding
None.

Availability of data and materials
Data will be made available upon request.

Declarations

Ethics approval and consent to participate
Not applicable.

Consent for publication
Not applicable.

Competing interests
The author's decalred that they have no competing interests.

Author details
[1]Rajarambapu College of Pharmacy Kasegaon, Sangli, Maharashtra 415404, India. [2]Eklavya College of Pharmacy Tasgaon, Sangli, Maharashtra 416312, India.

Received: 9 August 2023 Accepted: 2 December 2023
Published online: 20 December 2023

References

1. Bharadwaj R, Haloli J, Medhi S (2019) Topical delivery of methanolic root of *Annona reticulata* against skin cancer. S Afr J Bot 124:484–493. https://doi.org/10.1016/j.sajb.2019.06.006
2. Gopalakrishnan T, Ganapathy S, Veeran V, Namasivayam N (2019) Preventive effect of D-carvone during DMBA induced mouse skin tumorigenesis by modulating xenobiotic metabolism and induction of apoptotic events. Biomed Pharmacother 111:178–187. https://doi.org/10.1016/j.biopha.2018.12.071
3. Gupta AK, Browne M, Bluhm R (2002) Imiquimod: a review. J Cutan Med Surg 6:554–560. https://doi.org/10.1007/s10227-001-0134-6
4. Caperton C, Berman B (2019) Safety efficacy, and patient acceptability of imiquimod for topical treatment of actinic keratoses. Clin Cosmet Investig Dermato 14:35–40. https://doi.org/10.2147/ccid.s14109
5. Abbas O, Abadi R, Hanna E (2016) Imiquimod in dermatology: an overview. Int J Dermat 55(831):844. https://doi.org/10.1111/ijd.13235
6. Severino P, Fangueiro JF, Ferreira SV, Basso R, Chaud MV, Santana MH, Rosmaninho A, Souto EB (2013) Nanoemulsions and nanoparticles for non-melanoma skin cancer: effects of lipid materials. Clin Transl Oncol 15(6):417–424. https://doi.org/10.1007/s12094-012-0982-0
7. Rai VK, Mishra N, Yadav KS, Yadav NP (2018) Nanoemulsion as pharmaceutical carrier for dermal and transdermal drug delivery: formulation development, stability issues, basic consideration and applications. J Control Rel 270:203–225. https://doi.org/10.1016/j.jconrel.2017.11.049
8. Somagoni J, Boakye CHA, Godugu C, Patel AR, Faria M, Zucolotto V, Singh M (2014) Nanomiemgel: a novel drug delivery system for topical application—in vitro and in vivo evaluation. PLoS ONE 9(12):1–30. https://doi.org/10.1371/journal.pone.0115952
9. Silva HD, Poejo J, Pinheiro AC, Donsì FF, Serra AT, Duarte CMM, Ferrari G, Cerqueira MA, Vicente AA (2018) Evaluating the behaviour of curcumin nanoemulsions and multilayer nanoemulsions during dynamic in vitro digestion. J Funct Foods 48:605–613. https://doi.org/10.1016/j.jff.2018.08.002
10. Zhou H, Yue Y, Liu G, Li Y, Zhang J, Gong Q, Yan Z, Duan M (2010) Preparation and characterization of a lecithin nanoemulsion as a topical delivery system. Nanoscale Ress Lett 5(1):224–230. https://doi.org/10.1007/s11671-009-9469-5
11. Babu RJ, Pawar KR (2014) Lipid materials for topical and transdermal delivery of nanoemulsion. Crit Rev Ther Drug Carrier Syst 31(5):429–458. https://doi.org/10.1615/critrevtherdrugcarriersyst.2014010663
12. Telò I, Pescina S, Padula C, Santi P, Nicoli S (2016) Mechanisms of imiquimod skin penetration. Int J Pharm 511(1):516–523. https://doi.org/10.1016/j.ijpharm.2016.07.043
13. Kim S, Abdella S, Abid F, Afinjuomo F, Youssef SH, Holmes A, Song Y, Vaidya S, Garg S (2023) Development and optimization of Imiquimod loaded nanostructured lipid carriers using a hybrid design of experiments approach. Int J Nanomed 18:1007–1029. https://doi.org/10.2147/IJN.S400610
14. Algahtani MS, Ahmad MZ, Nourein IH, Ahmed J (2020) Co delivery of Imiquimod and curcumin by nanoemulgel for improved topical delivery and reduced psoriasis like skin lesions. Biomolecules 10(7):968. https://doi.org/10.3390/biom10070968
15. Panonnummal R, Shammika P, Aiswarya S, Gopikrishnan A, Jayakumar R, Sabitha M (2019) Chaulomoogra oil-based methotrexate loaded topical nanoemulsion for the treatment of psoriasis. J Drug Deliv Sci Technol 49:463–476. https://doi.org/10.1016/j.jddst.2018.12.020
16. Sharma P, Tailang M (2020) Design, optimization and evaluation of hydrogel of primaquine loaded nanoemulsion for malaria therapy. Fut J Pharmaceut Sci 6:1–11. https://doi.org/10.1186/s43094-020-00035-z
17. Shah V, Gandhi K, Parikh R, Sharma M, Suthar V (2016) Quality by design approach for optimization of microemulsion based topical gel. Marm Pharmaceut J 20:415–424. https://doi.org/10.12991/mpj.20162084614
18. Patil O, Manjappa A, Kumbhar P, Bhosale S, Disouza J, Salawi A, Sambamoorthy U (2022) Development of stable self-nanoemulsifying composition and its nanoemulsion for improved oral delivery of non-oncology drugs against hepatic cancer. Open Nano 7:1–15. https://doi.org/10.1016/j.onano.2022.100044
19. Norazlinaliza S, Garcia-Celma MJ, Escribano E, Nolla J, Llinas M, Basri M, Solans C, Esquena J, Tadros T (2018) Formulation of nanoemulsion containing Ibuprofen by PIC method for topical delivery. Mater Today Proc 5:S172-179
20. Kaplana UAB, Cetina M, Orgulb D, Taghizadehghalehjoughi A, Hacımuftuoglud A, Hekimoglub S (2019) Formulation and in-vitro evaluation of topical nanoemulsion and nanoemulsion-based gels containing daidzein. J Drug Deliv Sci Technol 52:189–203. https://doi.org/10.1016/j.jddst.2019.04.027
21. Avasatthi V, Pawar H, Dora CP, Bansod P, Singh Gill M, Suresh S (2016) Novel nanogel formulation of methotrexate for topical treatment of psoriasis: optimization, in vitro and in-vivo evaluation. Pharm Dev Technol 21(5):554–562. https://doi.org/10.3109/10837450.2015.1026605
22. Honmane S, Chimane S, Bandgar S, Patil S (2020) Development and optimization of Capecitabine loaded nano liposomal system for cancer delivery. Ind J Pharmaceut Edu And Res 54:376–384
23. Lu WC, Huang DW, Wang C-CR, Yeh CH, Tsai JC, Huang YuT, Li PH (2018) Preparation, characterization, and antimicrobial activity of nanoemulsions incorporating citral essential oil. J Food Drug Anal 26(1):82–89. https://doi.org/10.1016/j.jfda.2016.12.018
24. Harrison LI, Stoesz JD, Battiste JL, Nelson RJ, Zarraga IE (2009) A pharmaceutical comparison of different commercially available imiquimod 5% cream products. J Dermatolog Treat 20(3):160–164. https://doi.org/10.1080/09546630802513693
25. Bramhankar DM, Jaiswal SB (2009) Controlled release medication. Biopharmaceutics and pharmacokinetics: a treatise, 2nd edn. Vallabh Prakashan, pp 432–433
26. Paulo C, Sousa Lobo JM (2001) Modeling and comparison of dissolution profiles. Eur J Pharm Sci 13(2):123–133. https://doi.org/10.1016/S0928-0987(01)00095-1
27. Chime SA, Onunkwo GC, Onyishi II (2013) Kinetics and mechanisms of drug release from swellable and non swellable matrices: a review. Res J Pharm Biol Chem Sci 4(2):97–103
28. Shejawal KP, Randive DS, Bhinge SD, Bhutkar MA, Wadkar GH, Todkar SS, Mohite SK (2020) Functionalized single walled carbon nanotube for colon targeted delivery of isolated lycopene in colorectal cancer: in-vitro cytotoxicity and in-vivo roentgenographic study. J Mater Res 36:4894–4907. https://doi.org/10.1557/s43578-021-00431-y
29. Shejawal KP, Randive DS, Bhinge SD, Bhutkar MA, Todkar SS, Mulla AS, Jadhav NR (2021) Green synthesis of silver, iron and gold nanoparticles of lycopene extracted from tomato: their characterization and cytotoxicity

against COLO320DM, HT29 and hella cell. J Mater Sci Mater Med 32:1–12. https://doi.org/10.1007/s10856-021-06489-8
30. Randive DS, Gavade AS, Shejawal KP, Bhutkar MA, Bhinge SD, Jadhav NR (2021) Colon targeted dosage form of Capecitabine using folic acid anchored modified carbon nanotube: in-vitro cytotoxicity, apoptosis and in vivo roentgenographic study. Drug Dev Ind Pharm 47(9):1401–1412. https://doi.org/10.1080/03639045.2021.1994988
31. Kamble RV, Bhinge SD, Mohite SK, Randive DS, Bhutkar MA (2021) *In-vitro* targeting and selective killing of mcf-7 and colo320dm cells by 5-fluorouracil anchored to carboxylated SWCNTs and MWCNTs. J Mater Sci Mater Med 32(6):1–15. https://doi.org/10.1007/s10856-021-06540-8
32. Chavan RR, Bhinge SD, Bhutkar MA, Randive DS, Wadkar GH, Todkar SS, Urade MN (2020) Characterization, antioxidant, antimicrobial and cytotoxic activities of green synthesized silver and iron nanoparticles using alcoholic *Blumea erianthan* DC plant extract. Mater Today Commun. https://doi.org/10.1016/j.mtcomm.2020.101320
33. Jindal A, Kumar A (2022) Physical characterization of clove oil based self-nanoemulsifying formulations of cefopodaxime proxetil: Assessment of dissolution rate, antioxidant and antibacterial activity. Open Nano 8:100087. https://doi.org/10.1016/j.onano.2022.100087
34. Pereira Oliveira CN, Nani Leite M, de Paula NA, Araújo Martins Y, Figueiredo SA, Cipriani Frade MA, Lopez RFV (2023) Nanoemulsions based on sunflower and rosehip oils: the impact of natural and synthetic stabilizers on skin penetration and an ex vivo. Pharmaceutics 15(3):1–24. https://doi.org/10.3390/pharmaceutics15030999
35. Schimtt S, Schafer UF, Dobler L, Reichling J (2010) Variation of in-vitro skin permeation of rose oil between different application sites. Forsch Komplementmedm 17(3):126–310. https://doi.org/10.1159/000315043
36. Elkomy MH, Elmenshawe SF, Eid HM, Ali AM-A (2016) Topical ketoprofen nanogel: artificial neural network optimization, clustered bootstrap validation and in vivo activity evaluation based on longitudinal dose response modelling. Drug Deliv 23(9):3294–3306. https://doi.org/10.1080/10717544.2016.1176086
37. Sarheed O, Dibi M, Ramesh KVRNS (2020) Studies on the effect of oil and surfactant on the formation of alginate-based o/w lidocaine nanocarriers using nanoemulsion template. Pharmaceutics 12(12):1223. https://doi.org/10.3390/pharmaceutics12121223
38. Capek I (2013) Nanosuspensions. In: Tadros T (ed) Encyclopedia of colloid and interface science. Springer, Berlin, pp 748–782. https://doi.org/10.1007/978-3-642-20665-8_28
39. Bruschi ML (2015) Mathematical models of drug release. Strategies to modify the drug release from pharmaceutical systems, 1st edn, Woodhead Publishing UK. pp 63–86

Publisher's Note